

Hybrid Reactor Simulation of Boiling Water Reactor Power Oscillations

Zhengyu Huang & Robert M. Edwards

To cite this article: Zhengyu Huang & Robert M. Edwards (2003) Hybrid Reactor Simulation of Boiling Water Reactor Power Oscillations, Nuclear Technology, 143:2, 132-143, DOI: [10.13182/NT03-A3403](https://doi.org/10.13182/NT03-A3403)

To link to this article: <https://doi.org/10.13182/NT03-A3403>



Published online: 10 Apr 2017.



Submit your article to this journal [↗](#)



Article views: 10



View related articles [↗](#)

HYBRID REACTOR SIMULATION OF BOILING WATER REACTOR POWER OSCILLATIONS

REACTOR SAFETY

KEYWORDS: boiling water reactor, oscillation, simulation

ZHENGYU HUANG and ROBERT M. EDWARDS*
The Pennsylvania State University
The Department of Mechanical and Nuclear Engineering
228 Reber Building, University Park, Pennsylvania 16802-1408

Received September 13, 2001

Accepted for Publication September 11, 2002

Hybrid reactor simulation (HRS) of boiling water reactor (BWR) instabilities, including in-phase and out-of-phase (OOP) oscillations, has been implemented on The Pennsylvania State University TRIGA reactor. The TRIGA reactor's power response is used to simulate reactor neutron dynamics for in-phase oscillation or the fundamental mode of the reactor modal kinetics for OOP oscillations. The reactor power signal drives a real-time boiling channel simulation, and the calculated reactivity feedback is in turn fed into the TRIGA reactor via an experimental changeable reactivity device. The thermal-hydraulic dynamics, together with first harmonic mode power dynamics, is digitally simulated in the real-time environment. The real-time digital simulation of boiling channel thermal hydraulics is performed by solving constitutive equations for different regions in the channel

and is realized by a high-performance personal computer. The nonlinearity of the thermal-hydraulic model ensures the capability to simulate the oscillation phenomena, limit cycle and OOP oscillation, in BWR nuclear power plants. By adjusting reactivity feedback gains for both modes, various oscillation combinations can be realized in the experiment. The dynamics of axially lumped power distribution over the core is displayed in three-dimensional graphs. The HRS reactor power response mimics the BWR core-wide power stability phenomena. In the OOP oscillation HRS, the combination of reactor response and the simulated first harmonic power using shaping functions mimics BWR regional power oscillations. With this HRS testbed, a monitoring and/or control system designed for BWR power oscillations can be experimentally tested and verified.

I. INTRODUCTION

Boiling water reactor (BWR) power oscillation is an instability phenomenon that occurs under certain conditions, i.e., low core flow and relatively high power. There are two kinds of oscillations: in-phase or global oscillation, during which the average reactor core power oscillates periodically, and out-of-phase (OOP) or regional oscillation, during which the power in one half of the reactor oscillates out of phase against the other half (power of one half increases while the other half decreases and vice versa). Because reactor power oscillations may compromise the reactor fuel design safety margin, these instability phenomena call for special concerns among both utilities and nuclear regulatory agencies.¹ Extensive

works, both analytically and experimentally, have been done to study the mechanisms and to digitally simulate these instability phenomena.²⁻⁸ Monitoring and control techniques have been developed within academic and industrial domains.^{9,10} Most monitoring and control techniques are developed on the basis of theoretical analysis where various assumptions and simplifications are necessitated. Rigorous reactor models with details can be used to test and verify these designs. An effective alternative is to develop a hybrid simulation system in which partial or the entire reactor system can be simulated with physical systems. For a BWR system, neutron dynamics can be substituted with a research reactor and/or the thermal hydraulics of the boiling channel can be simulated by a thermal-hydraulic test facility.

The techniques described in this paper provide a relatively more realistic method for testing and verification

*E-mail: rmenuc@engr.psu.edu

of stability monitoring and control techniques by taking into account real-world characteristics of physical systems, instrumentation, and digital implementations. The hybrid simulations described here are the extension of the work done by Turso et al.¹¹ The hybrid simulation in this context refers to the use of the physical time response of the research reactor as an input signal to a real-time simulation of power reactor thermal hydraulics that in turn provides a feedback signal to the reactor through positioning of an experimental changeable reactivity device (ECRD). In this sense, this hybrid reactor simulation (HRS) system is also complementary to the hybrid system described by Kok and Van Der Hagen,¹² in which boiling channel thermal hydraulics is obtained from a physical thermal-hydraulic loop and the reactor physics is simulated digitally.

The new version of HRS is capable of simulating both in-phase and OOP oscillations that have occurred in BWR nuclear power plants. Instead of using linear reduced-order thermal-hydraulic models for boiling channels, thermal-hydraulic models containing mass, energy, and momentum equations are employed. By using these detailed thermal-hydraulic models, most two-phase flow phenomena such as subcooled boiling, transient boiling, bulk boiling, void distribution, and different types of two-phase flow pressure drops are modeled in detail. The model is free from the limitations imposed previously by the boiling channel linear feedback model.¹¹ During the implementation of the HRS, the constitutive equations are solved with the finite difference method in a C-MEX S-function under the Mathwork's Real-Time Workshop. Preliminary implementation of the HRS shows that both kinds of oscillations can be replicated by tuning the reactivity feedback gains.

II. BWR DYNAMICS MODEL DESCRIPTION

The dynamic model of boiling channels used in this research is basically taken from the research of BWR stability monitoring done by Ceceñas-Falcón⁹ and Ceceñas-Falcón and Edwards.¹³ Following is a review of this model.

The model has three parts as follows:

1. *neutron kinetics*: including point kinetics for in-phase oscillation and modal kinetics for OOP oscillation
2. *fuel dynamics*: identical for in-phase and OOP oscillation
3. *boiling channel thermal-hydraulic dynamics*: basically the same for both types of oscillation except for boundary conditions.

The model can accept any axial power shape in the reactor. The unevenly heated boiling channels are evenly divided into 24 nodes within each of which lumped mod-

els are used for fuel dynamics and boiling channel mass, energy, and momentum equations.

II.A. Neutron Kinetics

The models used for two types of oscillation are different: point kinetics is used for in-phase oscillation, and modal kinetics is used for OOP oscillation.

II.A.1. Point Kinetics Model

Point kinetics equations with one-delayed neutron group are used to simulate an in-phase oscillation problem:

$$\frac{dn_r}{dt} = \frac{\rho - \beta}{\Lambda} n_r + \frac{\beta}{\Lambda} c_r \quad (1)$$

and

$$\frac{dc_r}{dt} = \lambda(n_r - c_r) , \quad (2)$$

where n_r and c_r are normalized neutron and precursor density.

II.A.2. Modal Kinetics Model

First-order truncated modal expansion of time- and spatial-dependant neutron density is expressed as

$$\Psi(\underline{r}, t) = n_{0r}(t)\phi_0(\underline{r}) + n_{1r}(t)\phi_1(\underline{r}) , \quad (3)$$

where

$n_{0r}(t)$ = normalized fundamental mode neutron density

$n_{1r}(t)$ = first harmonic mode neutron density

$\phi_0(\underline{r})$ = shape function for the fundamental mode

$\phi_1(\underline{r})$ = shape function for the first harmonic mode.

$\phi_0(\underline{r})$ and $\phi_1(\underline{r})$ have the following expressions:

$$\phi_0(r, z, \theta) = J_0\left(2.40 \frac{r}{R}\right) \sin\left(\pi \frac{z}{H}\right) \quad (4)$$

and

$$\phi_1(r, z, \theta) = J_1\left(3.83 \frac{r}{R}\right) \sin\left(\pi \frac{z}{H}\right) \sin(\theta) , \quad (5)$$

where

J_0 = Bessel function of order 0

J_1 = Bessel function of order 1.

The dynamics of the neutron densities of the two modes are governed by the following four differential equations:

$$\frac{dn_{0r}}{dt} = \frac{(\rho_0 - \beta)}{\Lambda_0} n_{0r} + \frac{\rho_1}{\Lambda_0} n_{1r} + \frac{\beta}{\Lambda_0} c_{0r} , \quad (6)$$

$$\frac{dc_{0r}}{dt} = \lambda n_{0r} - \lambda c_{0r} , \quad (7)$$

$$\frac{dn_{1r}}{dt} = \frac{(\rho_1^s + \rho_0 - \beta)}{\Lambda_1} n_{1r} + \frac{\rho_1}{\Lambda_1} n_{0r} + \frac{\beta}{\Lambda_0} c_{1r} , \quad (8)$$

and

$$\frac{dc_{1r}}{dt} = \frac{\Lambda_0}{\Lambda_1} \lambda n_{1r} - \lambda c_{1r} , \quad (9)$$

where

c_{0r} = precursor density of fundamental mode

c_{1r} = precursor density of first harmonic mode

ρ_1^s = subcriticality of the first harmonic mode.

II.B. Fuel Dynamics

For each node, fuel and clad temperatures are lumped node-average variables. Only radial heat transfer, from the rod to clad by conduction and from clad to fluid by convection, is considered due to the comparatively negligible axial heat conduction effect. Energy balance equations for fuel rod and clad in each node are respectively expressed as follows:

$$m_f c_{pf} \frac{d\bar{T}_f}{dt} = q'(t) - \frac{1}{R'_g} [\bar{T}_f(t) - \bar{T}_c(t)] \quad (10)$$

and

$$m_c c_{pc} \frac{d\bar{T}_c}{dt} = \frac{1}{R'_g} [\bar{T}_f(t) - \bar{T}_c(t)] - \frac{1}{R'_c} [\bar{T}_c(t) - \bar{T}_m(t)] , \quad (11)$$

where

\bar{T}_f, \bar{T}_c = node average temperatures

R'_g = thermal resistance per node of fuel

R'_c = thermal resistance per node of cladding.

II.C. Boiling Channel Thermal Hydraulics

The thermal-hydraulic dynamics model is basically the same for the fundamental mode and the first harmonic mode, except that different boundary conditions are applied. Three regions of single phase, subcooling boiling, and bulk boiling are considered in the model. By neglecting the effect on energy change of varying pres-

sure change and of channel wall friction, constitutive equations for mass, energy, and momentum are expressed respectively as follows:

$$\frac{\partial \rho_m}{\partial t} + \frac{\partial G_m}{\partial z} = 0 , \quad (12)$$

$$\rho_m \frac{\partial h_m}{\partial t} + G_m \frac{\partial h_m}{\partial z} = \frac{q'' P_h}{A_z} , \quad (13)$$

and

$$\frac{\partial G_m}{\partial t} + \frac{\partial}{\partial z} \left(\frac{G_m^2}{\rho_m} \right) = -\frac{\partial p}{\partial z} - \frac{f G_m |G_m|}{2 D_e \rho_m} - \rho_m g . \quad (14)$$

The coolant in the boiling channel is assumed to be incompressible ($\partial \rho_m / \partial p = 0$), but the density is specified as a function of enthalpy at a certain pressure. Thus, we have

$$\frac{\partial \rho_m}{\partial t} = \frac{\partial \rho_m}{\partial h_m} \bigg|_p \frac{\partial h_m}{\partial t} + \frac{\partial \rho_m}{\partial p} \bigg|_{h_m} \frac{\partial p}{\partial t} = R_h \frac{\partial h_m}{\partial t} . \quad (15)$$

By combining Eqs. (12), (13), and (15), local mass flow along the channel has the following form:

$$\frac{\partial G_m}{\partial z} = -R_h \left(\frac{q'' P_h}{A_z} - G_m \frac{\partial h_m}{\partial z} \right) . \quad (16)$$

Together with system pressure information, Eq. (13) is used to determine equilibrium quality distribution and thus flow quality distribution. Void fraction distribution is determined through the following void-quality relation:

$$\alpha = \frac{x \rho_f}{s(1-x)\rho_g + x \rho_f} , \quad (17)$$

where s is slip ratio, which is a function of flow conditions.⁹

Pressure drop along the boiling channel is the sum of pressure drops in each node contributed by gravity, acceleration, and friction. For in-phase oscillation and for the fundamental mode of OOP oscillation, this pressure drop is coupled with a simple first-order recirculation dynamics; for the first harmonic mode of OOP oscillation, the total pressure drop across the reactor core is forced to be constant—the same as that established in the steady-state condition, by adjusting inlet mass flow rate.

II.D. Coupling Between Neutron Dynamics and Thermal Hydraulics

Boiling channel thermal hydraulics is coupled to the neutron dynamics through Doppler and void reactivity feedback. Reactivity terms in Eqs. (1), (6), and (8) (ρ , ρ_0 , and ρ_1 , respectively) have the following common format:

$$\rho = \rho_{ext} + \rho_D + \rho_\alpha, \quad (18)$$

where ρ_{ext} mainly refers to the reactivity change caused by the control rods, which is not considered in this research; ρ_D and ρ_α are Doppler reactivity feedback and void reactivity feedback, respectively. Doppler reactivity ρ_D reflects the effect of fuel temperature change on the neutron density and is expressed as:

$$\rho_D = D(\bar{T}_f - \bar{T}_{f0}) \quad (19)$$

and the void reactivity feedback ρ_α is calculated by a plant-specific empirical correlation (ρ_{ac}) and weighted by the square of axial power distribution:

$$\rho_{ac} = -0.0108 - 0.0207\alpha + 0.140\alpha^2 - 0.135\alpha^3 \quad (20)$$

and

$$\rho_\alpha = \frac{\int_0^H \Phi^2(z) \rho_{ac}(z) dz}{\int_0^H \Phi^2(z) dz}, \quad (21)$$

where Eq. (20) is taken from the paper by March-Leuba and Otaduy-Bengoa.¹⁴

III. HRS EXPERIMENTAL SETUP

The hybrid reactor simulation in this research is an extension from the study performed by Turso et al.¹¹ and

by Edwards et al.¹⁵ The key feature of HRS is that full or part of the neutron dynamics is simulated with a real reactor, instead of by solving differential equations. Besides the computer hardware and software upgrades,¹⁵ the main change lies on the fuel temperature dynamics and boiling channel thermal-hydraulics simulation, which are here simulated using first-principle constitutive equations as described in Secs. II.B and II.C, respectively. For in-phase oscillation, the reactor point kinetics is obtained from the reactor physical response; while for OOP oscillation, the fundamental mode dynamics is with the reactor, but the first harmonic mode neutron dynamics is still simulated digitally.

III.A. In-Phase Oscillation HRS Setup

The setup of HRS for in-phase oscillation is shown in Fig. 1.

In this setup, the Penn State Breazeale Reactor (PSBR) is used to supply the key signal—reactor power—to the digital simulation.¹⁵ By using this signal, the digital simulation calculates BWR fuel temperature and channel thermal-hydraulic responses—temperature distribution within the fuel and void distribution within the boiling channel. Reactivity feedback is calculated on the basis of these results and fed back to the reactor by positioning of an ECRD. An ECRD is an aluminum tube containing absorber material that is positioned within the central thimble of the reactor by an experimental setup. One important upgrade of current HRS over the original HRS¹¹ is that the worth and the reactivity change

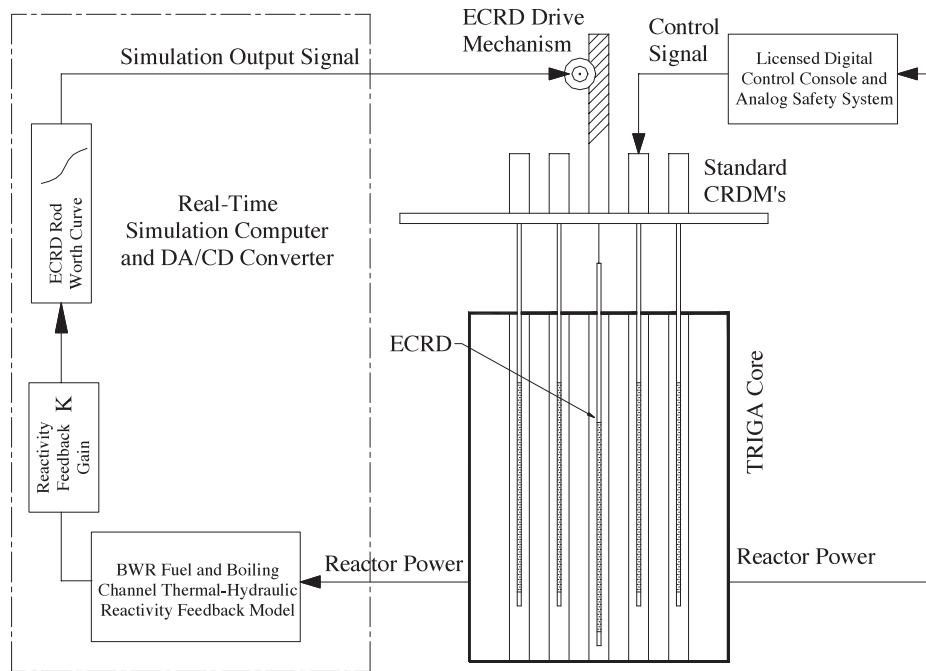


Fig. 1. In-phase oscillation HRS setup.

rate of the current ECRD (ECRD #2) is about three times greater than the original one (ECRD #1)—0.94 \$ versus 0.35 \$ for reactivity and 0.35 \$/s versus 0.12 \$/s for reactivity change rate.

The channel simulation calculates pressure drop, temperature, and void fraction distribution in the channel on the basis of the governing equations (mass, energy, and momentum equations). The reactivity feedback of Doppler-Effect (temperature feedback) and void distribution change is calculated and then converted to the ECRD movement. After multiplied by a feedback gain K , namely bifurcation factor, to take into account many factors encountered in real plants, the calculated reactivity change rate is sent to the reactor in the form of speed demand signal (voltage) to control the ECRD movement on the basis of ECRD worth curve.¹¹

The digital simulation part is implemented under MATLAB Real-Time Workshop (RTW) by an AMD 1-MHz PC with 373 megabytes RAM. The processor is fast enough to deal with the detailed boiling channel thermal-hydraulic simulation. A National Instruments data acquisition card is installed in the AMD computer to collect data from the reactor. The outgoing control signal is connected to the ECRD control device via a DAC card. By compromising between the simulation accuracy, which requires fine time-step, and real-time simulation requirement, which limits refining simulation time-step, the time-step is set to 0.05 s. The simulation, including user interface and thermal hydraulic calculation, is implemented with MATLAB Simulink¹⁶ and MATLAB RTW (Ref. 17). The thermal-hydraulic calculation is coded in a C-MEX S-function required by RTW.

III.B. OOP Oscillation

Compared with in-phase oscillation, the OOP oscillation experiment setup¹⁸ is more complicated because of more simulation components—first harmonic neutron dynamics and thermal hydraulics for both fundamental and first-harmonic modes. Many factors, such as more interactions among these components, the heavier computational task, and frequent generation of three-dimensional (3-D) graphs, result in more computational burden. To address this problem, a three-computer configuration is used together with the PSBR to form the current OOP oscillation HRS system. The block diagram showing the composition of the HRS system and the relationship among its components is shown in Fig. 2, where the reactor and each computer are represented in their corresponding individual blocks.

Three computers employed in this system are as follows:

1. *Host computer*: The simulation is developed in the host computer in the MATLAB Simulink¹⁶ environment. Before the experiment, the Simulink program is compiled to generate an executable code, which is down-

loaded to the target computer, under MATLAB Real-Time Workshop.¹⁷ During the experiment, the principal user interaction takes place on this host computer where parameter adjustments are initiated and some elementary information displays are presented—this computer is used as the experiment control terminal. Start and termination of the experiment and evolution of oscillations are controlled from this computer.

2. *Target computer*: Before the experiment, the executable code is downloaded in this computer from the host computer; during the experiment, all digital simulation and the reactor control signal calculation are implemented here.

3. *Graphic computer*: Three-dimensional BWR power distribution is vividly displayed in real-time based on the experimentally measured reactor power (the fundamental mode power, in the context of HRS) and the simulated first harmonic mode power.

The host computer and target computer work cooperatively under the MATLAB RTW environment through Ethernet connection. Communication between the target computer and the graphic computer is via serial cable connection. The TRIGA reactor is interfaced with the target computer via a National Instruments data acquisition card.

The HRS is implemented mainly with the TRIGA reactor and the target computer. The TRIGA reactor is used to simulate BWR fundamental mode power dynamics, while the first harmonic mode power, together with fuel temperature dynamics and detailed thermal hydraulics of boiling channels of both fundamental mode and first harmonic mode, is simulated digitally in real time in the target computer. Simulations of boiling channels provide reactivity feedback, which is the combination of Doppler reactivity feedback due to fuel temperature change and the void reactivity feedback due to void distribution change, to the TRIGA reactor. The TRIGA reactor's power response is in turn fed into the channel simulations and the first harmonic mode power simulation. The digital simulations of the boiling channel thermal hydraulics and the first harmonic neutron dynamics are implemented with C-MEX S-functions. The differential equations of fuel temperature dynamics and boiling channel thermal hydraulics are solved with the finite difference method.¹³ Due to the restriction of fixed-step integration in real-time implementation, the prompt jump approximation¹⁹ is applied in the "first harmonic mode neutron dynamics" block.

A fast 3-D display of reactor power distribution is implemented using MATLAB graphics capability. During the experiment, the measured reactor power (the fundamental mode reactor power, in the context of OOP HRS) and the simulated first harmonic mode power are transferred to this computer, and then the axially lumped reactor power distributions are calculated on the basis of

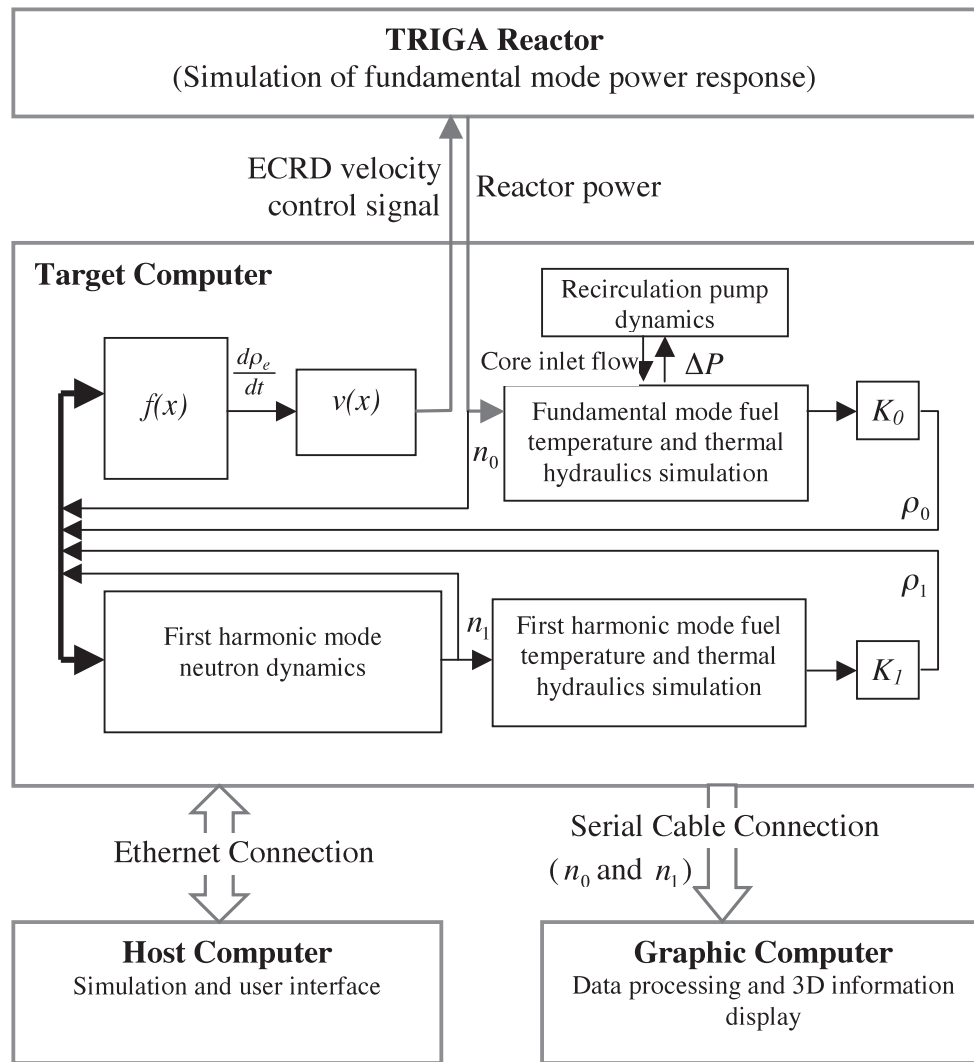


Fig. 2. Composition of OOP HRS system and relationship of its components.

these two variables. Three-dimensional graphs representing fundamental, first harmonic, and the combination of these two with Eqs. (3), (4), and (5) are generated and displayed in this computer. These graphs are updated in real-time every 0.125 s (at a frequency of 8 Hz).

The target computer performs boiling channel thermal-hydraulic and the first harmonic mode power simulations and the control of the ECRD in the TRIGA reactor. The TRIGA reactor power is measured, and a control signal is sent to the ECRD drive mechanism to simulate the BWR reactivity feedback. Desired hybrid simulation of BWR behavior is controlled by adjusting parameters in the host computer.

Similar to the in-phase oscillation HRS, reactivity feedback gains, K_0 and K_1 in Fig. 2, are introduced to take into account uncertainties of the reactor system such as the fuel burnup, reactor aging or recirculation flow failure, the characteristics of reactor core,

etc., and used to adjust the system stability characteristics—to make it stable, in-phase oscillating or OOP oscillating.

In Fig. 2, the reactor works together with the sub-component blocks $f(x)$ and $v(x)$ in the target computer block to simulate the fundamental mode power dynamics described in Eq. (6). The function block $f(x)$ takes the power of and the reactivity feedback from the fundamental mode and first harmonic mode to generate the equivalent reactivity feedback ρ_e and then its derivative $d\rho_e/dt$. Generation of ρ_e is based on the following observations.

Rewriting of Eq. (6) yields:

$$\frac{dn_{0r}}{dt} = \frac{\left(\left(\rho_0 + \frac{n_{1r}}{n_{0r}} \rho_1 \right) - \beta \right)}{\Lambda_0} n_{0r} + \frac{\beta}{\Lambda_0} c_{0r} \quad (22)$$

Comparing Eq. (22) with Eq. (1), if we write

$$\rho_e = \rho_0 + \frac{n_{1r}}{n_{0r}} \rho_1, \quad (23)$$

then Eq. (22) has the same form as Eq. (1). Therefore, ρ_e can be used as input signal to drive the ECRD.

In the block $f(x)$, Eq. (23), together with the time-derivative algorithm, is implemented. The block of $v(x)$ implements the signal conversion function where the derivative of reactivity input is converted into the ECRD speed demand signal (driving voltage to the ECRD drive mechanism).¹¹

III.C. Implementation of HRS

Because of the large temperature feedback of PSBR above 10 KW, the reactor must be operated at a low power level at which the temperature rise is not high enough to result in noticeable TRIGA reactor reactivity feedback. To run HRS, the nominal power is set to 500 W.

An experiment consists of three main steps. First, the reactor is brought to 500 W by the licensed reactor control console. Second, with the aid of the main console automatic control, the ECRD is positioned to the vertical center by the experimental setup while the reactor power is maintained at 500 W. During these two steps, the reactor power measurement is connected to the fuel temperature dynamics and boiling channel thermal hydraulics, but the calculated Doppler and void reactivity

feedback is not fed back to the reactor. Finally, after the reactor power is stabilized, the reactor power control is switched to the experiment control but under the close monitoring of the licensed reactor operator. Because of the parameter difference between the physical system and the data used for digital simulation, the critical values of feedback gains of the experiment may be different from those of pure digital simulation, so these gains are carefully adjusted from very small values to bring the reactor HRS to in-phase or OOP oscillation.

IV. DEMONSTRATION OF SIMULATION RESULTS AND ANALYSIS

Presented in this section are the results from the two sets of BWR oscillation experiment setup for in-phase and OOP oscillations. Section IV.A presents in-phase oscillation results, and Sec. IV.B focuses on OOP oscillation results even though in-phase oscillation is within the simulation capability of the OOP oscillation HRS setup merely by setting $K_1 = 0$.

IV.A. In-Phase Oscillation

Figure 3 shows the results from the HRS using La-salle BWR parameters at the initial power of 45% nominal power with the bifurcation factor $K = 0.68$. At about 2518 s, the ECRD speed demand (see the first plot)

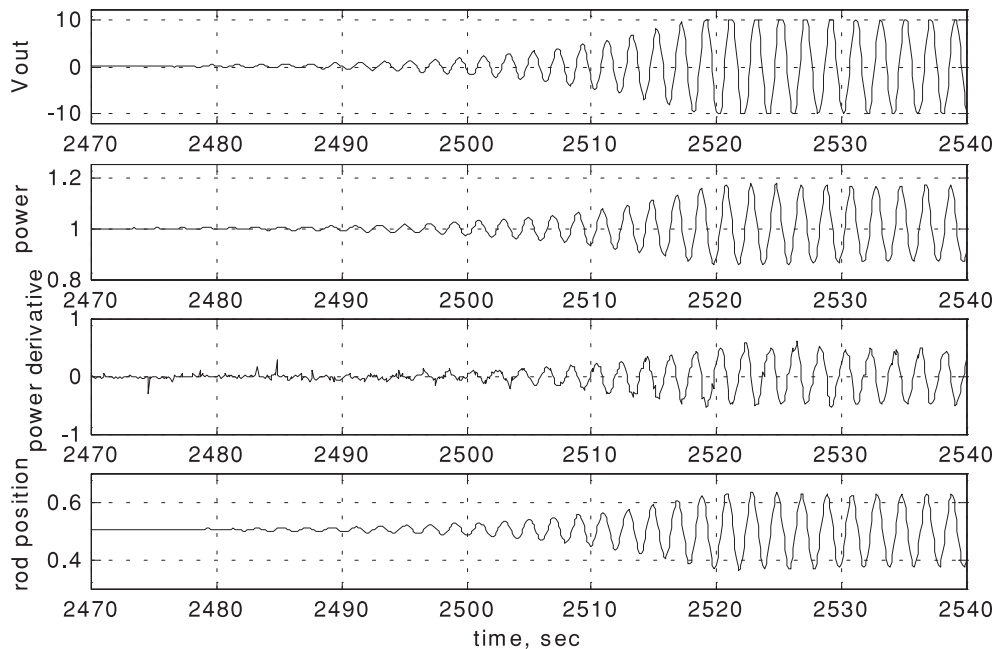


Fig. 3. In-phase oscillation HRS results. The first plot from the top: ECRD speed demand signal; second plot: reactor power relative to the 45% nominal power; third plot: reactor power change rate; bottom plot: ECRD position (1, fully withdrawn; 0, fully inserted).

reaches its limit (± 10 V) so the reactivity feedback gain K is set to its critical value $K_0 = 0.63$ to force the system to oscillate at a constant magnitude. During the period shown in this figure, a pseudo-limit cycle evolution is presented. During the limit cycle, the ECRD speed demand signal system reaches saturation (± 10 V) where the power oscillates from 88.5 to 119% of its initial value (see the second plot). The third plot shows the power change rate. The bottom plot shows the ECRD position during the oscillation. Position 1 means the ECRD is fully withdrawn, while position 0 means fully inserted. From this plot it is clear that the ECRD moves only a little over one-quarter of its full length during the limit cycle even though the rod reactivity change rate has saturated. Running digital simulation with a reactivity step change of -0.01 \$ (detailed results are not presented here) shows that the fully developed limit cycle requires the reactivity change rate of ± 0.70 \$/s and a total reactivity of 0.42 \$. The ECRD used in this experiment has a maximum reactivity change rate of about 0.35 \$/s and a total reactivity worth of 0.94 \$. So the limit of ECRD capacity is not from its reactivity worth but its change rate.

The measured reactor power fluctuation range is approximately $\pm 11\%$ of its steady-state value, which is much larger than that obtained by Turso et al.¹¹ due to ECRD upgrade. It is expected that with a possible further upgraded ECRD the fully developed limit cycle with oscillation amplitude of 60 to 70% steady-state value,

which has been observed in real power plants, will be able to be simulated without artificial suppression by adjusting reactivity feedback gain K .

Phase portrait of power signal (power change rate versus power) is shown in Fig. 4. Although further development of the limit cycle is suppressed by adjusting bifurcation factor K , the nonlinearity of the system is illustrated in this figure by the asymmetry about the vertical centerline.

IV.B. OOP Oscillation

Figure 5 shows the results from a hybrid simulation of OOP oscillation using Vermont Yankee plant parameters. Physical experiment at Vermont Yankee demonstrated in-phase behavior only²⁰; but to demonstrate the methodology of OOP simulation, the OOP feedback gains were artificially made large enough in this work to induce simulated OOP behavior. (Vermont Yankee characteristics may not allow such an oscillation behavior.) Shown in the figure are the fundamental mode and first harmonic mode power responses of the case that the fundamental mode oscillation is merely excited by the first harmonic mode oscillation. During the time range shown in the figure, the fundamental mode reactivity feedback gain K_0 is set well below its critical value. At 1190 s, the first harmonic mode reactivity feedback gain K_1 was changed to an above-critical value (0.6) to initiate the first harmonic mode power oscillation. K_1 was

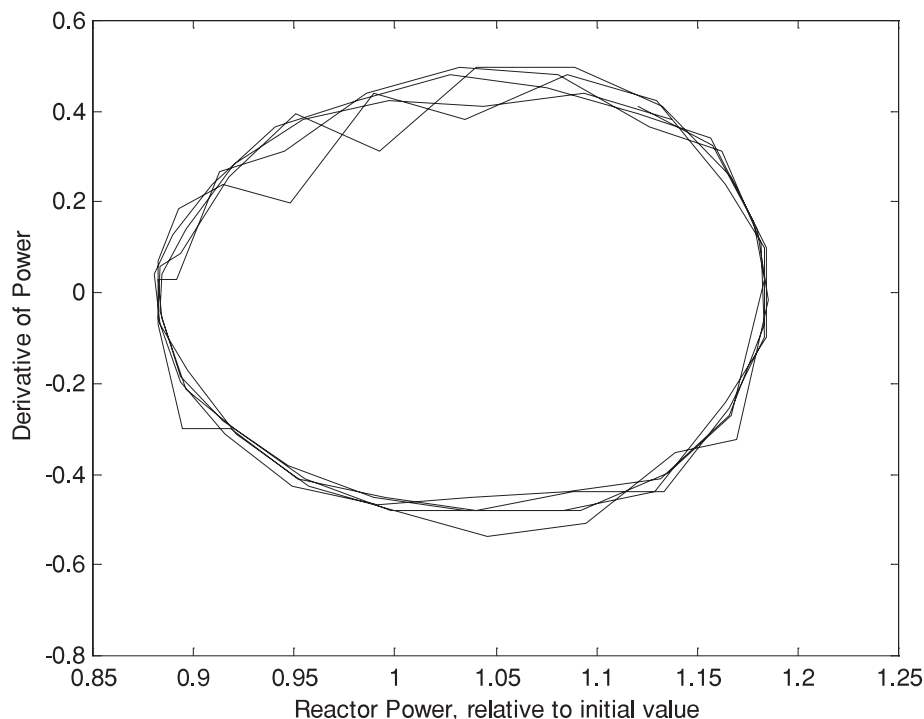


Fig. 4. Phase portrait of reactor power of in-phase oscillation HRS experiment.

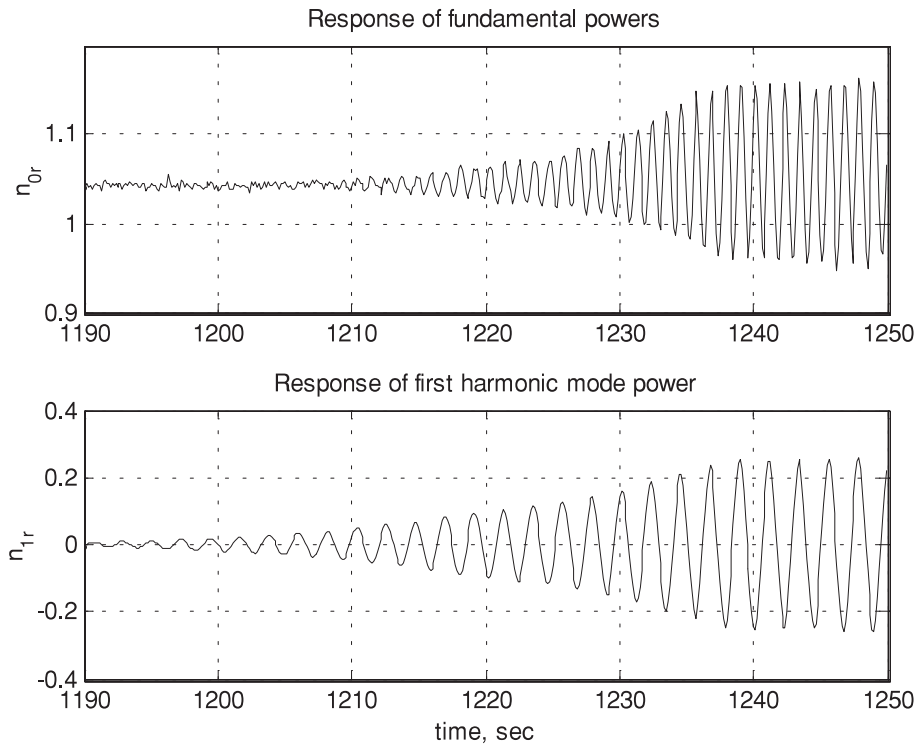


Fig. 5. OOP oscillation power responses.

set to a lower value (but still above critical value) at 1220 s and was then gradually decreased to its critical value (0.38) to maintain the constant magnitude oscillation and prevent the ECRD moving to speed saturation. Theoretically, the magnitude of OOP oscillation can be stabilized (limit cycle is reached) without changing reactivity feedback gain due to the nonlinear characteristics of the system. However, the capacity of the ECRD limits the further evolution of the oscillation—its velocity saturates before limit cycle is fully developed.

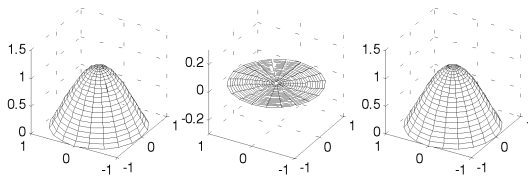
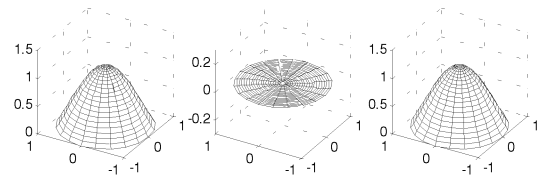
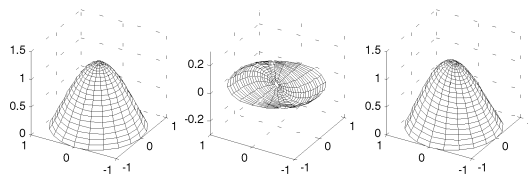
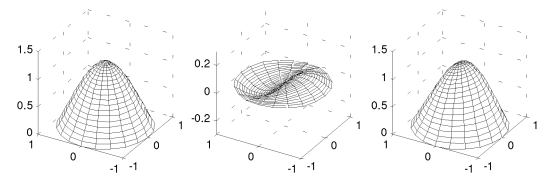
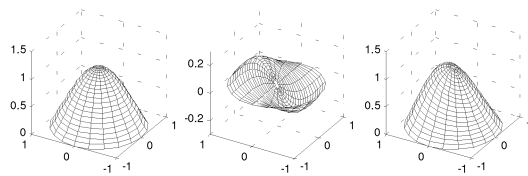
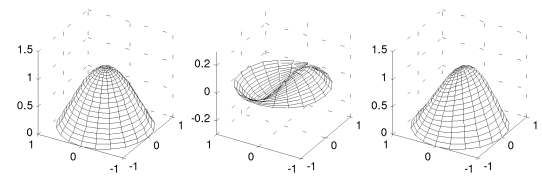
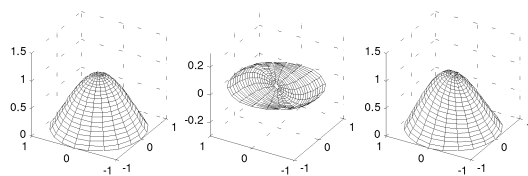
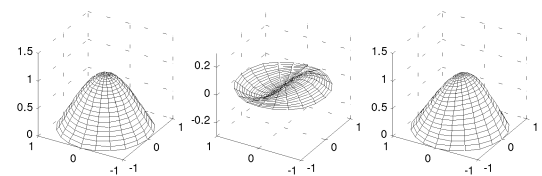
Prior to 1210 s, no obvious oscillation is observed in the fundamental mode power (reactor power), even though the first harmonic mode power oscillation has started since 1190 s. The roughness presented in the figure is due to reactor and measurement noise. After 1210 s, the fundamental mode power starts to oscillate, and its magnitude grows significantly so that actions must be taken such as decreasing K_1 to suppress its further evolution. Obviously, the fluctuation of the fundamental mode power is excited by the first harmonic mode power oscillation instead of its inherent unstable characteristics—strictly speaking, the overall system is unstable regardless of which oscillation starts first.

Besides this cross-mode excitation, another feature is the relationship between the oscillation frequencies of the two modes. In Fig. 5, the periods of the fundamental mode and first harmonic mode oscillations are 1.15 and 2.3 s, respectively, i.e., the fundamental mode power os-

cillates at a frequency twice that of the first harmonic mode. This is the consequence of the coupling effect of the neutron dynamics of the two modes. The second term in the right side of Eq. (6), the production of first harmonic mode power and its reactivity feedback, is the excitation to the fundamental mode. The production of two identical-frequency terms results in a double frequency oscillation of the fundamental mode as demonstrated by Farawila.²¹ The oscillation frequency ($f = \frac{1}{2.3} = 0.43$ Hz) is exactly the same as that observed during the Vermont Yankee plant test, which was an in-phase experiment.²⁰

The peak-to-peak amplitude of the oscillation is about 18 and 50% of the steady-state values for fundamental mode and first harmonic mode, respectively. The fundamental mode power oscillation amplitude is roughly the same as that recorded during the Vermont Yankee nuclear power plant oscillation test indicating that, though the ECRD needs to be upgraded, current HRS setup is capable to simulate some instability events.

Shown in Fig. 6 are a series of 3-D displays of the reactor power over one oscillation cycle (for first harmonic mode, the period is $T = 2.3$ s; for the fundamental mode, the period is $T/2$). The three columns, from left to right, correspond to fundamental mode, first harmonic mode, and the combined power distributions of a bare homogeneous cylindrical reactor for which Eqs. (3), (4), and (5) are applied. These graphs are reproduced to represent

a) $t = t_0$

e) $t = t_0 + T/2$

b) $t = t_0 + T/8$

f) $t = t_0 + 5T/8$

c) $t = t_0 + T/4$

g) $t = t_0 + 3T/4$

d) $t = t_0 + 3T/8$

h) $t = t_0 + 7T/8$


Note:

Starting time: $t_0=1236.5$ sec
Oscillation period: $T=2.3$ sec
($T/2$ for fundamental mode)

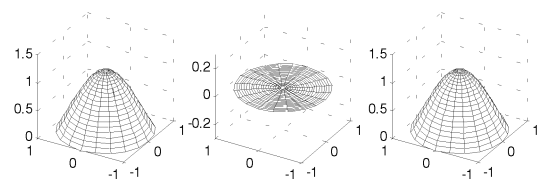
i) $t = t_0 + T$


Fig. 6. Three-dimensional representation of reactor power distribution during one cycle of OOP oscillation. Column 1, fundamental mode; column 2, first harmonic mode; column 3, combined power.

the displays on the graphic computer during the time period of [1236.5 1238.8] s corresponding to Fig. 5.

V. SUMMARY AND FUTURE WORK

Two sets of experimental setup have been established to simulate power oscillation events of BWR power plants using a university research reactor and first-

principle boiling channel models under MATLAB RTW. Two types of oscillations, namely in-phase and OOP oscillations that have been observed in BWR plants, can be simulated by adjusting reactivity feedback gain(s). The characteristics of the experimental results agree with nuclear power plant observations; therefore, the fidelity of the HRS system is verified. This system can be used to test and verify BWR control and stability monitoring techniques.

Future work includes expanding the current hybrid system to incorporate a BWR boiling channel thermal-hydraulic test loop to simulate the boiling channel thermal hydraulics of the fundamental mode. The test loop and the reactor will be electronically coupled to simulate BWR oscillation phenomena. Finally, BWR oscillation monitoring and control techniques will be tested.

NOMENCLATURE

A_z = flow area
 C_{pc} = cladding specific heat
 C_{pf} = fuel specific heat
 G_m = mixture mass flux
 H = reactor height
 h_m = mixture enthalpy
 k = thermal conductivity
 m_c = cladding mass
 m_f = fuel mass
 P_h = heated perimeter
 q' = linear power rate
 q'' = heat flux
 R = reactor radius
 r = radial position
 S = slip ratio
 T_c = cladding temperature
 T_f = fuel temperature
 T_m = coolant mean temperature
 t = time
 x = flow quality
 x_e = equilibrium quality
 z = axial position

Greek

α = void fraction
 β = delayed neutron fraction
 δ = gap width
 θ = azimuthal angle
 Λ = neutron life time
 λ = precursor decay constant
 ρ = reactivity

ρ_0 = fundamental mode reactivity
 ρ_1 = first harmonic mode subcriticality
 ρ_1^s = first harmonic mode reactivity
 ρ_α = void reactivity
 ρ_{ac} = empirical reactivity feedback correlation
 ρ_D = Doppler reactivity
 ρ_{ext} = external reactivity
 ρ_f = saturated liquid density
 ρ_g = saturated vapor density
 ρ_m = mixture density
 Φ = axial power shape

ACKNOWLEDGMENT

This research is sponsored by U.S. Department of Energy Nuclear Engineering Education and Research project DE-FG07-99ID13778.

REFERENCES

1. "General Design Criteria for Nuclear Power Plants: Criterion 12—Suppression of Reactor Power Oscillations," 10CFR50, Appendix A, *Code of Federal Regulations*.
2. J. MARCH-LEUBA, D. G. CACUCI, and R. B. PEREZ, "Nonlinear Dynamics and Stability of Boiling Water Reactors: Part 1—Qualitative Analysis," *Nucl. Sci. Eng.*, **93**, 111 (1986).
3. J. MARCH-LEUBA, D. G. CACUCI, and R. B. PEREZ, "Nonlinear Dynamics and Stability of Boiling Water Reactors: Part 2—Quantitative Analysis," *Nucl. Sci. Eng.*, **93**, 124 (1986).
4. J. MARCH-LEUBA, "A Reduced-Order Model of Boiling Water Reactor Linear Dynamics," *Nucl. Technol.*, **75**, 15 (1986).
5. J. MARCH-LEUBA and E. D. BLAKEMAN, "A Mechanism for Out-of-Phase Power Instabilities in Boiling Water Reactors," *Nucl. Sci. Eng.*, **107**, 173 (1991).
6. Y. TAKEUCHI, Y. TAKIGAWA, and H. UEMATSU, "A Study on Boiling Water Reactor Regional Stability from the Viewpoint of Higher Harmonics," *Nucl. Technol.*, **106**, 300 (1994).
7. J. A. TURSO, M. MARCH-LEUBA, and R. M. EDWARDS, "A Modal-Based Reduced-Order Model of BWR Out-of-Phase Instabilities," *Ann. Nucl. Energy*, **24**, 921 (1997).
8. D. HENNING, "A Study on Boiling Water Reactor Stability Behavior," *Nucl. Technol.*, **126**, 10 (1999).
9. M. CECENAS-FALCÓN, "Stability Monitoring for Boiling Water Reactors," PhD Thesis, The Pennsylvania State University (May 1999).

10. C. M. MOWRY, I. NIR, and D. W. NEWKIRK, "Operational Control of Boiling Water Reactor Stability," *Nucl. Technol.*, **109**, 412 (1995).
11. J. A. TURSO, R. M. EDWARDS, and J. MARCH-LEUBA, "Hybrid Simulation of Boiling Water Reactor Dynamics Using a University Research Reactor," *Nucl. Technol.*, **110**, 132 (1995).
12. H. V. KOK and T. H. J. VAN DER HAGEN, "Design of a Simulated Void-Reactivity Feedback in a Boiling Water Reactor Loop," *Nucl. Technol.*, **128**, 1 (1999).
13. M. CECENAS-FALCÓN and R. M. EDWARDS, "Stability Monitoring Tests Using a Nuclear-Coupled Boiling Channel Model," *Nucl. Technol.*, **131**, 1 (2000).
14. J. MARCH-LEUBA and P. J. OTADUY-BENGOA, "A Comparison of BWR Stability Measurements with Calculations Using the Code LAPUR-IV," NUREG/CR-2998, ORNL/TM-8546, Oak Ridge National Laboratory (1983).
15. R. M. EDWARDS, Z. HUANG, and W. HE, "Integration of a Thermal-Hydraulic Test-Loop and University Research Reactor for Advanced Monitoring and Control Research," *Proc. Int. Topl. Mtg. Nuclear Plant Instrumentation, Control and Human-Machine Interface Technologies (NPIC & HMIT 2000)*, Washington, D.C., November 13–16, 2000, American Nuclear Society (2000).
16. *SIMULINK Dynamic System Simulation for MATLAB*, Version 4, The Mathworks (2000).
17. *Real Time Workshop for Use with Simulink*, Version 4, The Mathworks (1999).
18. R. M. EDWARDS and Z. HUANG, "Hybrid Reactor Simulation and 3-D Information Display of BWR Out-of-Phase Oscillation," *Trans. Am. Nucl. Soc.*, **84**, 99 (2001).
19. D. L. HETRICK, *Dynamics of Nuclear Reactors*, The University of Chicago Press, Chicago (1971).
20. S. A. SANDOZ and S. F. CHEN, "Vermont Yankee Stability Tests During Cycle 8," *Trans. Am. Nucl. Soc.*, **45**, 754 (1983).
21. Y. M. FARAWILA, "Application of Modal Neutron Kinetics to Boiling Water Reactor Oscillation Problems," *Nucl. Sci. Eng.*, **129**, 261 (1998).

Zhengyu Huang (BS, marine power engineering, 1988, and MS, reactor engineering and reactor safety, 1991, Harbin Shipbuilding Engineering Institute, China; MS, electrical engineering, The Pennsylvania State University (Penn State), 2001; PhD, nuclear engineering, Penn State, 2002) is currently an engineer at Thermoflow, Inc. His industrial experience includes software development for power plant design, nuclear power plant safety system design, and nuclear cogeneration plant heat balance analysis. His current research interest includes power plant control using modern control technologies.

Robert M. Edwards (BS, nuclear engineering, Penn State, 1971; MS, nuclear engineering, University of Wisconsin, 1972; PhD, nuclear engineering, Penn State, 1991) is a professor in the Department of Mechanical and Nuclear Engineering at Penn State. Previously, he was the director of software development at LeMont Scientific. In the early 1970s, he was employed at General Atomic. His research interests are in control and simulation.